Removal of the phthalocyanine dye from acidic solutions using resins with the polystyrene divinylbenzene matrix

D. Kaušpėdienė*,

E. Kazlauskienė,

R. Česūnienė,

A. Gefenienė,

R. Ragauskas,

A. Selskienė

*Institute of Chemistry
of Center for Physical
Sciences and Technology,
A. Goštauto 9,
LT-01108 Vilnius,
Lithuania*

Two resins of polystyrene divinylbenzene matrix: the macroporous strong base Purolite A 500PS anion exchanger and hypercrosslinked non-functionalized Macronet MN 200 were proofed as suitable adsorbents for the removal of hazardous copper phthalocyanine dye – Acid Blue 249 (CuPc). The sorption isotherms and kinetics of CuPc in acidic aqueous solutions were investigated using batch experiments. The resins surface texture was evaluated using a scanning electron microscope. The FTIR study of unloaded and CuPc dye loaded resins identified the functional groups of resins and dye anion and the specific sorption mechanisms: ion exchange in participation of the protonated quarternary amino groups of Purolite A 500P and the electrostatic interaction in participation of the fenolic groups of Macronet MN 200. The kinetic data were correlated with intraparticle diffusion and the pseudo-second order kinetic equations. The activation energies such as intraparticle diffusion (E_{a-k_1}) and chemical sorption (E_{a-k_2}) were calculated using the Arrhenius relationship. The CuPc dye sorption on Purolite A 500PS is limited by the intraparticle diffusion, whereas sorption on Macronet MN 200 is limited by the intraparticle diffusion depending on pore size distribution and on the boundary layer thickness.

Purolite A 500PS is substantially more effective for the sorption of CuPc dye than Macronet MN 200. The amount of CuPc dye sorbed at equilibrium on Purolite A 500PS and on Macronet MN 200 was 86.9 µmol/g and 2.3 µmol/g, respectively.

Key words: sorption, polymeric sorbent, copper phthalocyanine dye, kinetic

INTRODUCTION

The extensive use of metal complex dyes in various industries often poses pollution problems as in colored wastewater discharged into environmental water bodies as well as from the carcinogenic properties of mainly used in dyes metals, chromium, cobalt, copper, and amines formed by reductive cleavage of azo groups of organics [1, 2]. Dye removal, in particular, has recently become an area of major scientific interest, where the adsorption is considered to be one of the most effective methods and a proven technology that has applications for water reuse in the industry. Its superiority over other techniques can be assessed in terms of initial costs, flexibility and simplicity of design, ease of operation, intensity to toxic pollutants, and the advantage of not leading to harmful products [1, 2].

Adsorption of dye using ion exchange resins is a practical method for the removal of dyes from wastewaters and recycling water when compared with the widely used adsorption onto activated carbon. Its main advantages are as follows: the ion exchangers are not lost during the regeneration, recovery of the process water, and the removal of soluble dye.

As there exists a large variety of dyes and their removal is based on dye-sorbent interaction that depends on the number and type of functional groups or the chemical and physical structures of matrix and on the structure of dye, the performance of sorbents should be thoroughly evaluated. The removal of acid and reactive dyes using different anion exchangers (strong and weak basic with gel or macroporous structures of styrene-divinylbenzene or acrylic matrices) was described in [3–9]. In some cases the proposed ion-exchange mechanisms were not predominant and some other mechanisms, e. g. repulsion between the dye molecules and / or

repulsion between the anion exchange matrix and the dye molecules, play an important role.

The properties of the ion exchanger depend on the nature of functional groups, the properties of the matrix of the initial inert polymer and its transformation during grafting the functional groups [10]. The polystyrenic skeletons obtained by suspension polymerization have a notable physical and chemical stability and are used by all manufacturers to obtain a large variety of ion exchangers by grafting different functional groups. This type of matrix is still the most important one because styrene monomer is relatively cheap and abundantly available. The macroporous polystyrenic polymers have permanent porosity due to phase separation arising during polymerization induced by the presence of a porogen in the reaction mixture. The corresponding ion exchangers compared with the gel ones have the advantage to exchange larger ions and are more resistant to fouling by organic matter present in natural surface water.

Hypercrosslinked polymeric adsorbents, including Macronets (Purolite International Ltd), have both macropores and micropores, the latter providing the high surface area and the former providing rapid access to the internal surfaces. The Macronet resins are relatively new commercial products obtained by Purolite, a third generation of polystyrenic resins, and are presented as alternatives to activated carbon [11–17]. These resins are obtained by post crosslinking the polymers swelled in a solvent in excess with conformational rigid bridges. These materials contain micro-, meso and macropores and have a large surface area. In addition, conventional ion-exchange functional groups can be attached to their matrix. The use of Macronets non-functionalized MN 200 and weak basic MN 300 for the dye (Acid Red 14) removal from a synthetic solution has been studied [18, 19]. The treatment of textile dye house waste streams using Macronets is a new industrial technology in development by Technocom through 5 operating plants in Italy [20] and the dye sorption mechanism is still being investigated.

The dye Acid Blue 249 chosen as a model adsorbate for the present study finds a wide application in the industry. The blue pigment copper(II) phthalocyanine (CuPc) and its derivative copper(II) phthalocyanine-3,4',4",4"'-tetrasulphonic acid tetrasodium salt are widely used in different industries such as enamels, plastics, textile, print inks, linoleum and rubber goods [21]. Furthermore, metal phthalocyanine derivatives exhibit high reduction and oxidation properties, since they have a molecular structure similar to that of porphyn. The electron transfer ability of metal phthalocyanine derivatives is attributed to their π electron conjugation system in their molecular structure. The soluble copper phthalocyanine derivatives are used in the fabrication of organic donor / acceptor solar cells [22]. The metal phthalocyanine belongs to a class of chemically and thermally stable organic semiconductors, which are studied due to their application as photosensitizers [23] and chemical sensors [24–26].

However, the entrance of such dye molecules as pollutants in aquatic environment through the waste waters released from the above-mentioned industries demands effective methods for their removal [27]. Process water recycling requires a total decolorization and an extensive elimination of all organic and inorganic contents which concentrations are controlled by environmental regulations. However, the information was not found in literature about the phthalocyanine dye removal from aqueous solutions using styrene divinylbenzene matrix anion exchange and non-functionalized resins.

The main objective of the present work was to compare the sorption potential of the styrene divinylbenzene macroporous strong base Purolite A 500PS anion exchanger and that of the non-functionalized hypercrosslinked Macronet MN 200 for the removal of copper phthalocyanine dye (CuPc) from acidic aqueous solutions. The importance of polystyrene divinylbenzene matrix on the sorption mechanism and kinetics was considered.

MATERIALS AND METHODS

Materials

Two sorbents of polystyrene-divinylbenzene skeleton: macroporous anion exchanger Purolite A 500PS and hypercrosslinked non-functionalized Macronet MN 200 were applied in the sorption studies (Table 1).
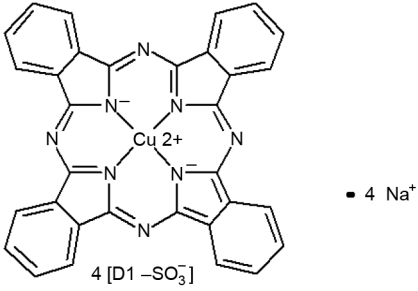
The anion exchanger Purolite A 500P was obtained in the Cl form. Conversion into the OH$^-$ form was carried out treating the resin sample in the column with 5 bed volumes (BV) of 4% NaOH at a flow rate of 4 mL/min (BV = the volume of treated solution / the volume of resin). After rinsing with distilled water for excess alkalinity in eluate the resin samples were sieved in the range of 0.5–0.7 mm. A sample of the Macronet MN 200 was conditioned in a methanol-hydrochloric acid mixture overnight, then washed and kept in distilled water before being used in the sorption experiments. Prior to experiments the samples of both sorbents were dried between filter sheets and weighed. Only a wet fraction of a narrow size range (0.5–0.7 mm) was used. The mass of dry sorbent used in calculations of the sorption capacities at equilibrium (q_e) and at time t (q_t) was predetermined with a separate sample of 0.5 g wet sorbent dried at 60 °C for 12 h. The sorption capacity values are presented in mmol per g of dry sorbent.

The characteristics of the copper phthalocyanine dye, which was used without further purification, are listed in Table 1. A series of experimental dye solutions in the concentration range 0.05 to 0.8 mmol/L of dye were obtained by successive dilution of 1 mmol/L stock solution. The pH values of initial solutions were measured and adjusted with 0.1 M HCl to pH 3.0 because Macronet MN 200 exhibits anion exchange properties at pH below 4.3 [12, 14].

Batch mode adsorption studies

Sorption isotherms and kinetics were determined by the batch method with a shaking speed of 400 rev/min^{-1}. The

Table 1. **Sorbents and dye properties**

Sorbent (The Purolite Company)	Anion exchanger Purolite A 500PS	Macronet MN 200
Polystyrene structure	Crosslinked	Hypercrosslinked
Physical form and appearance	Opaque spherical beads	Opaque spherical beads
Functional groups	R-N$^+$(CH$_3$)$_3$, Type 1 Quaternary Ammonium	Non-functionalized
Total capacity	Cl-form – 0.8 meq/ml	–
Moisture	63–70%	57–62%
Bead size range	0.425–1.2 mm with 2% max < 0.425 mm and 2% max > 1.2 mm	0.3–1.2 mm with 1% max < 0.3 mm and 5% max > 1.2 mm
Specific gravity	moist Cl-form 1.07 g/ml	1.04 g/ml
Shipping weight	640–670 g/l	700 g/l
Max. operating temperature	100 °C in Cl-form	100 °C
pH limits, stability	0–14	–
Specific surface area	25–70 m^2/g	800–1 000 m^2/g
Pore volume	0.379 ml/g	1.1 ml/g
Micropore volume	–	0.25 ml/g
Shrink / Swell Factor	15%	±5%
Dye characteristic (Sigma-Aldrich, Germany)		
CAS No.	27360-85-6	
Chemical name	Copper phthalocyanine tetrasulfonic acid tetrasodium salt (synonym: C. I. Acid Blue 249; Ariabel Blue 14.12; C. I. 74220; copperphthalocyaninetetrasulfonic acid tetrasodium salt; E 68; Heligon Blue S4; Heliogen Blue SBP; phthalocyanine tetrasulfonic acid tetrasodium salt coppercomplex; tetrasodium copper phthalocyaninetetrasulfonate; Cuprate(4-).	
Molecular structure		
Molecular formula	C$_{32}$H$_{12}$CuN$_8$O$_{12}$S$_4$4Na	
Molar weight	984.25 g/mol	

sorption isotherms were established by the change in the dye concentrations before and after the contact with the sorbent in an Erlenmeyer flask at 20.0 ± 0.1 °C until the adsorption equilibrium was reached. The equilibration time determined after adsorption studies at various time intervals was 120 min. Approximately 0.5 g of dry sorbent was added to 25 ml of the solution of a given initial concentration in the Erlenmeyer flask and equilibrated at shaking. After agitation, samples of 1 ml of the solution were taken out, and the residual concentration of dye was ascertained by an UV-Vis Spectrometer Cintra 101 (GBS Scientific Equipment (USA) LLS) at the respective λ_{max} value, which is 616 nm for this dye. The dye concentration was calculated from the calibration curve.

Kinetic curves were recorded when the samples of sorbent were equilibrated with 25 ml of 0.1 mmol L^{-1} dye solution at 293–303K during the predetermined time. Then the samples of the test solution (0.2 ml) were withdrawn and the residual concentration of dye determined.

The sorption capacities at equilibrium q_{eq} (mmol/g) and q_t at time t (mmol/g) were calculated by the following equation:

$$q_{eq(t)} = \frac{(C_0 - C_{e(t)})V}{W}, \quad (1)$$

where C_0 and C_e (or C_t) are the concentrations (mmol/L) of the dye in the solution before and after sorption, respectively,

V is the volume of the solution (L) and *W* is the mass of the dry anion exchanger (g).

The surface morphology of the adsorbents was studied by using a scanning electron microscope EVO 50EP (Carl Zeiss SMT AG) equipped with energy and wave dispersive X-ray spectrometers (Oxford Instruments) and a secondary electron detector (low vacuum mode, 10 kV, 50 Pa, working distance 10 mm).

IR-spectra of the adsorbents unloaded and loaded with dye were recorded by means of a FTIR spectrometer Perkin Elmer Instruments (LTEC) with a diamond cell: detector – MTC (Mercury-Cadmium-Telluride), source – MIR (Mid Infra-Red), resolution – 4.00 cm^{-1}, the number of scans – 50, turning the IR flux, wave range of 4 000–650 cm^{-1}.

RESULTS AND DISCUSSION

Effect of the initial dye concentration and pH

To determine the effect of the initial dye concentration and pH on the sorption process, the initial concentration of CuPc dye was varied from 0.05 mmol/L to 0.8 mmol/L. The CuPc dye sorption increased in proportion to the increase in the initial dye concentration at a fixed temperature and pH onto both the Purolite A 500PS macroporous anion exchanger (Fig. 1a) and the Macronet MN 200 (Fig. 1b). Although the specific surface and pore volume of Macronet MN 200 are 23.1 and 3.2 times higher, respectively (Table 1), than those of Purolite A 500PS, the amount of the sorbed CuPc dye per mass unit of the anion exchanger was higher when compared to that of non-functionalized Macronet MN 200. This can be explained by the presence of quaternary ammonium functional groups in Purolite A 500PS. The surface texture of both sorbents showed a similar globular structure (Fig. 2), where the globule diameter was approximately 300 nm, thus creating meso- and macropores which enable rapid diffusion of the dye molecule [14].

The pH had no effect on the CuPc dye sorption on the anion exchanger Purolite A 500PS: at pH values equal to 3.0 (not presented), 6.75 (Fig. 1a) and pH 9.25 (not presented) the uniform sorption capacity at the equilibrium was attained because the quaternary ammonium groups are ionic in both
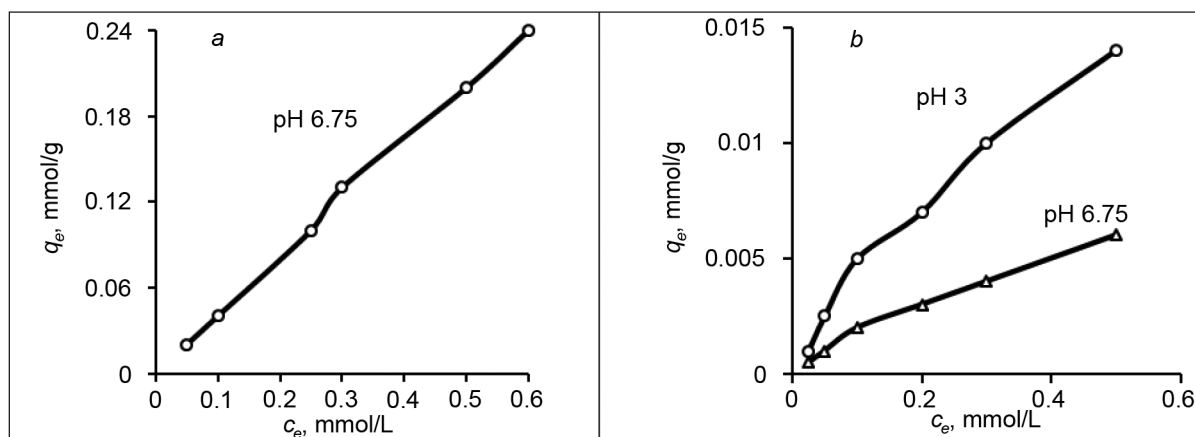

Fig. 1. Effect of initial dye concentration and pH on the sorption of CuPc dye on the anion exchanger Purolite A 500PS (*a*) and Macronet MN 200 (*b*). Conditions: mass of sorbent 0.5 g, contact time 120 min, shaking speed of 400 rev min^{-1}
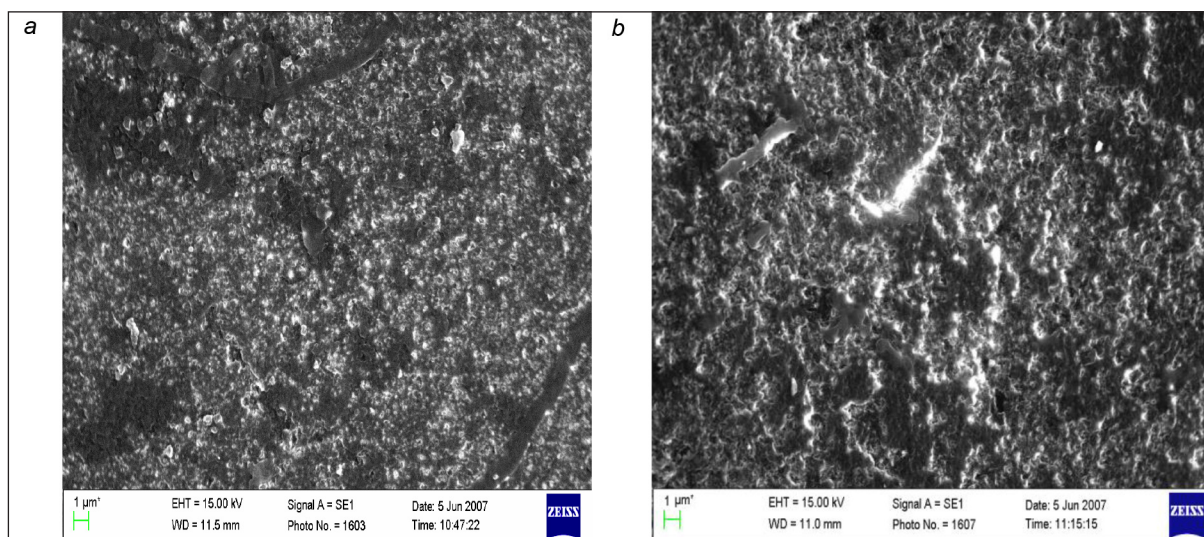

Fig. 2. Scanning electron micrographs of the bead cross-section of Purolite A 500PS (*a*) and Macronet MN 200 (*b*) at 10 000 × magnification

acidic and basic media (pK$_a$ = 2.31 [28]). The CuPc dye sorption onto Macronet MN 200 decreased with the increase in pH value (Fig. 1b).

The nature of binding between CuPc and Purolite A 500PS or Macronet MN 200 influenced their sorptive capacity. A detailed FTIR characterization of the unloaded strong basic anion exchanger Purolite A 500PS and that loaded with CuPc dye at optimized pH 3.0 at 20 °C temperature was carried out to identify the functional groups that are responsible for the dye sorption. In the recorded FTIR spectrum of dye CuPc (Fig. 3, Table 2) the characteristic peaks of 3 465 cm^{-1} (corresponding to NH groups), 1 591 cm^{-1} (corresponding to C=N groups), 1 420 cm^{-1} (corresponding to C=C groups) and 1 090 cm^{-1} (corresponding to the CN groups) [29] in the acidic medium are slightly shifted to a shorter wave field of 1 595 cm^{-1} (C=N), 1 421 cm^{-1} (C=C), 1 094 cm^{-1} (CN). The peaks at 1 020–1 040 cm^{-1} and 1 065–1 070 cm^{-1} are specific for the SO$_3^-$ groups present in the CuPc dye [29, 30].

In a high frequency region peak 3 384 cm^{-1} is very strong and a broad band of the O-H stretching vibration was observed both before sorption and after sorption of CuPc onto Purolite A 500PS (Fig. 3, Table 2). On the lower frequency side of this band some peaks at about 3 024, 2 925, 2 853 cm^{-1} appeared. The above mentioned peaks ascribed to the symmetric or asymmetric stretching vibration of the ring C-H bond and –CH$_2$ groups of the matrix of the dye loaded anion exchanger were virtually unchanged. It was therefore concluded that the polystyrene divinylbenzene matrix of the Purolite A 500PS is not participating in the sorption of CuPc dye. There was a spectral shift and the increased intensity of peaks in the area of functional groups NH and CN of the loaded with dye anion exchanger and new peaks at 1 020–1 040 cm^{-1} and 1 065–1 070 cm^{-1} characteristic of CuPc dye functional groups SO$_3^-$ appeared.

Consequently, one can assume that the dye CuPc sorption mechanism onto the anion exchanger Purolite A 500PS in the acidic medium may be attributed to the chemical reaction between the protonated quarternary amino groups (-N$^+$(CH$_3$)$_3$OH$^-$) of the anion exchanger and the dye anions (R'(SO$_3$)$_4^{4-}$) with accompaniment of the neutralization reaction:
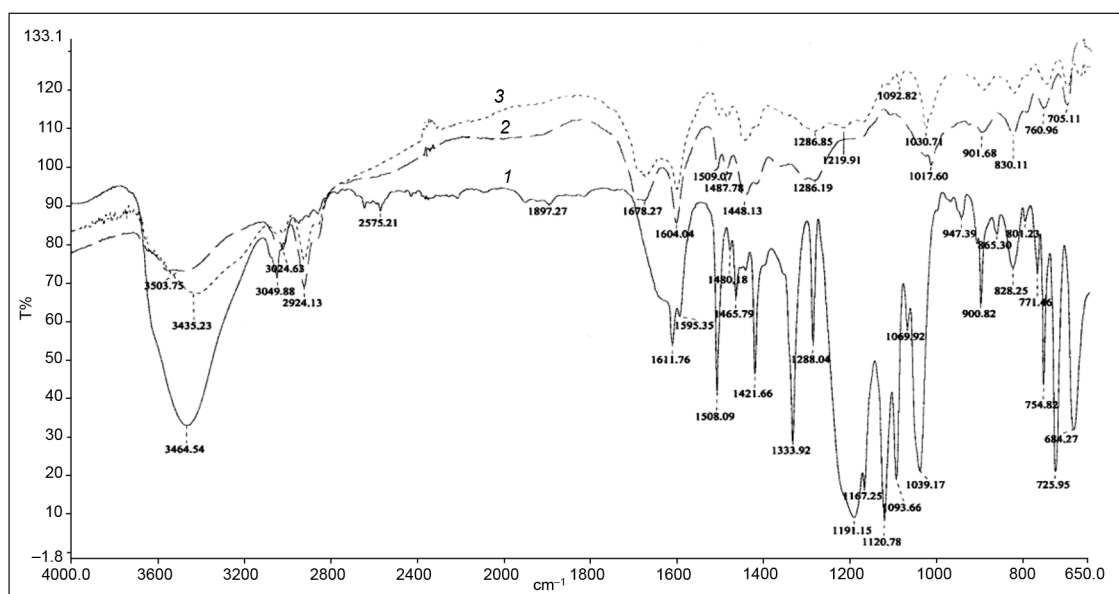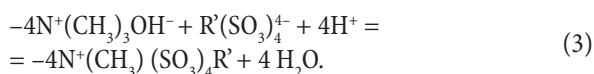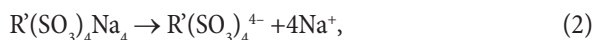

Fig. 3. FTIR spectra of CuPc dye (*1*), unloaded Purolite A 500PS (*2*) and Purolite A 500PS loaded with CuPc dye (*3*)

Table 2. **Wave number (cm^{-1}) for the dominant peak from FTIR for CuPc dye sorption onto Purolite A 500PS**

Functional groups	Dye CuPc	Purolite A 500 PS unloaded	Dye CuPc loaded Purolite A 500PS
OH		3 384	3 408
N-H	3 465		
C-H	3 050	3 024	3 024
C-H$_2$		2 925	2 925
		2 853	2 853
C-N	1 612		
	1 595		
C=C	1 421	1 426	1 426
C-N		1 222	1 221
	1 191		1 192
	1 093		1 091
SO$_3^-$	1 039		1 032

$$R'(SO_3)_4Na_4 \rightarrow R'(SO_3)_4{}^{4-} + 4Na^+, \tag{2}$$

$$-4N^+(CH_3)_3OH^- + R'(SO_3)_4{}^{4-} + 4H^+ =$$
$$= -4N^+(CH_3)(SO_3)_4R' + 4H_2O. \tag{3}$$

FTIR spectra of Macronet MN 200 show, as they do in the case of Purolite A 500PS, unchanged characteristic bands, attributable to the stretching vibrations of the >CH-. –CH$_2$- in the benzene ring and carbonyl functionality for both unloaded and dye loaded sorbent (Fig. 4, Table 3): the peak at 3 025 cm^{-1} corresponds to the stretching vibration of CH in the benzene ring, whereas the peak recorded at 2 924 cm^{-1} can be assigned to the vibration of aliphatic CH$_2$ and the peak at 1 678 cm^{-1} to the carbonyl groups (C=O) [14]. In the CuPc dye loaded Macronet MN 200 spectrum the shift in the wave number of the -OH group peak and highlights of the slightly altered characteristic peaks of CuPc dye can be seen: 3 025 cm^{-1} (NH), 1 093 cm^{-1} (CN) and 1 031 cm^{-1} (-SO$_3^-$).

These shifts in the wavelength of the dye loaded Macronet MN 200 FTIR spectrum showed that the dye binding process was taking place at the surface of the sorbent. This can be explained by the presence of 0.2 mmol/g phenolic groups on the surface of MN 200 beads from grafted or entangled chains of the surfactants employed in the suspension [12, 14, 31]. At pH lower than the total surface charges measured as point of zero charge pH$_{pzc}$ the presence of a considerable positive zeta potential on the MN 200 surface (pH$_{pzc}$ = 3.6 [31]) was attributed to the presence of oxygen in the framework of this adsorbent [12, 14]. The presence of these protonizable groups results in a partially hydrophilic character of the polymer structure that could be also favoring the sorption of anionic species present in the solution. The CuPc dye anion adsorption properties (electrostatic interaction) on Macronet MN 200 at pH < 3.6 were attributed to the following possibilities: $\rangle C = \overset{+}{O}H \leftrightarrow \rangle \overset{+}{C} - OH \leftrightarrow$ delocalized charge in the whole polymer framework.
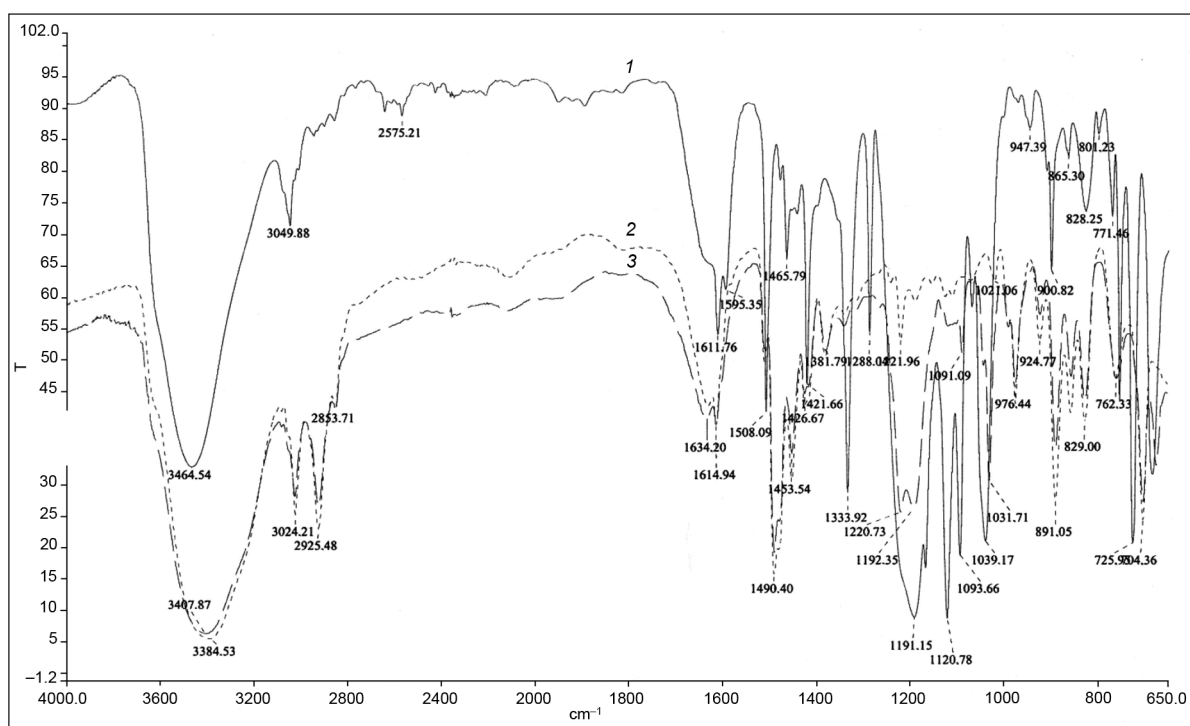

Fig. 4. FTIR spectra of CuPc dye (*1*), unloaded Macronet MN 200 (*2*) and Macronet MN 200 loaded with CuPc dye (*3*)

Table 3. **Wave number (cm^{-1}) for the dominant peak from FT-IR for CuPc dye sorption onto Macronet MN 200**

Functional groups	Dye CuPc	Macronet MN 200	Dye CuPc loaded Macronet MN 200
OH		3 504	3 435
N-H	3 465		
CH	3 050	3 025	3 025
CH$_2$		2 924	2 924
C-N	1 612		
	1 595		
C=O		1 678	1 678
		1 286	1 287
C-N	1 094		1 093
SO$_3^-$	1 039		1 031

Taking into account that FTIR showed the presence of protonizable groups, the sorption mechanism of CuPc onto the non-functionalized Macronet MN 200 surface ($>$S) could be described by the following reaction [18]:

$$>S + R'(SO_3)_4{}^{4-} + 4Na^+ \xleftrightarrow{\text{pH} \leq 3.6} >S \, R'(SO_3)_4 \, Na_4. \qquad (4)$$
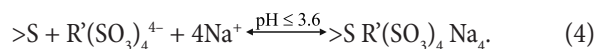
Kinetic studies

Kinetic studies were conducted to reveal the relation between the physical-chemical characteristics of the sorbents and their performance in the removal of CuPc dye. Kinetic parameters are also helpful for the determining the effectiveness of adsorbent and for designing and modeling the sorption process.

The time-dependent behavior of the dye adsorption was examined by varying contact time between the adsorbent and the dye solution in the range of 5–120 min. The amount of CuPc dye (q_t, mmol/L) plotted as a function of contact time t (Fig. 5a and Fig. 5b) showed that at the initial pH 3.0 and a constant temperature the equilibrium between the CuPc
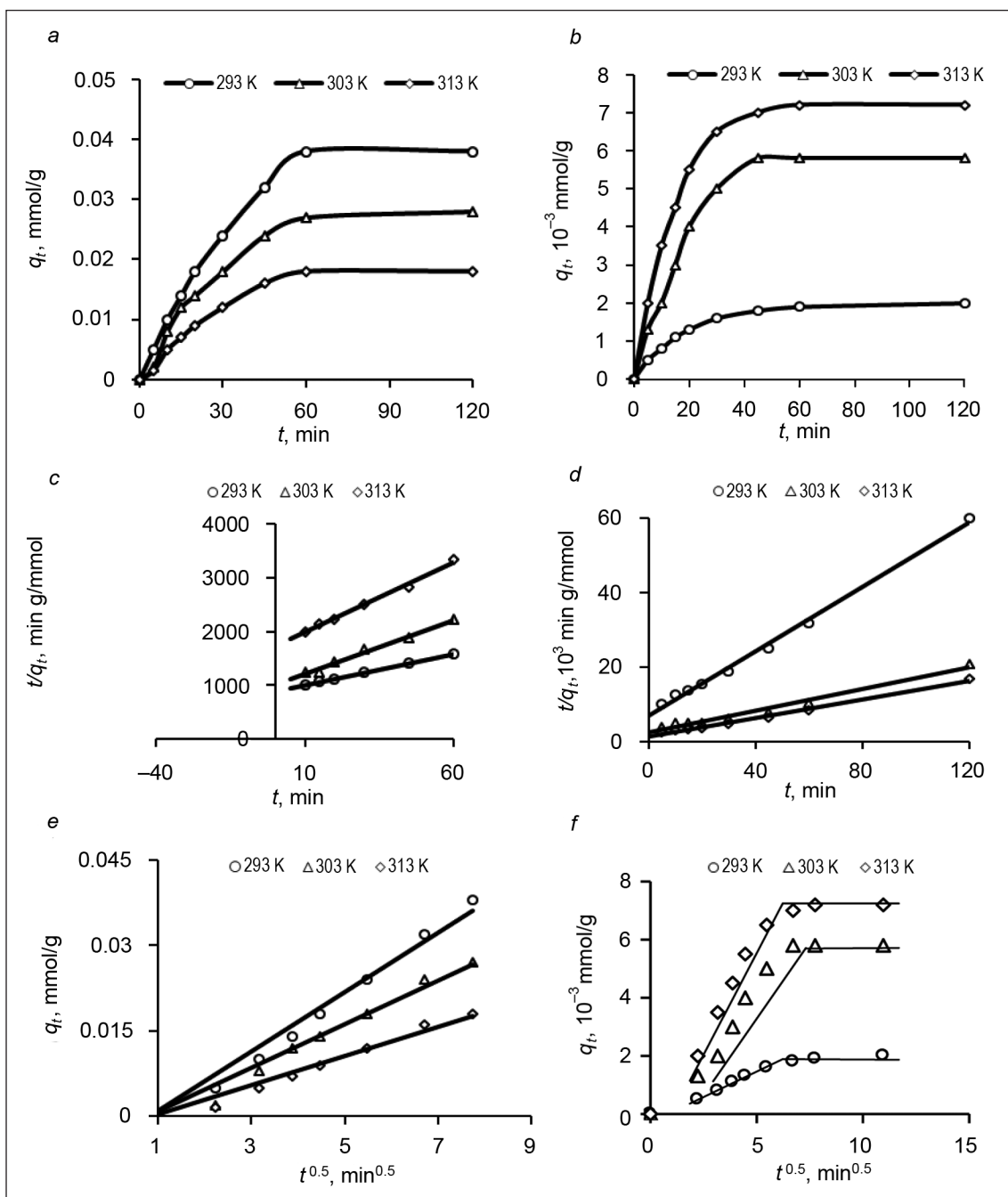

Fig. 5. Kinetic curves for the adsorption of CuPc dye on Purolite A 500PS (*a, c, e*) and Macronet MN 200 (*b, d, f*) at different temperatures: experimental (*a, b*); tests of pseudo-second-order reaction model equation (*c, d*) and intraparticle diffusion model equation (*e, f*). Conditions: mass of sorbent 0.5 g, initial CuPc dye solution concentration 100 μmol/l, pH 3.0; shaking speed of 400 rev/min⁻¹

dye and Purolite A 500PS was attained later (within shaking 60 min) than between the CuPc dye and Macronet MN 200 (within 45 min). From the obtained results it is clear that the course of sorption is rapid in the initial stage and becomes slow in later stages until equilibrium is attained. This is evident from the fact that a large number of surface sites are available for sorption at the beginning of the process, and, after a lapse of time, the remaining sites are difficult to occupy because of repulsion between CuPc dye molecules of the solid and bulk phases. A similar phenomenon was observed for the sorption of Tartrazine, Allura Red and Sunset Yellow on strong basic anion exchangers Amberlite IRA 900 and IRA 910 [5, 6].

Concerning the case of ion exchange, as several studies have demonstrated, it is basically a diffusion-controlled process and although it differs from adsorption they share many common aspects, enough to accept the use of the same simplified kinetic equations [32]. Analyses of the experimental kinetic data with two theoretical models (pseudo-second-order-reaction and intraparticle diffusion) were used to describe the CuPc dye sorption kinetics, and, simultaneously, to determine both the sorption rate and diffusion constants.

The pseudo-second-order rate model was selected because there is no need to know the equilibrium capacity from the experiments, as it can be calculated from the model [33]. The initial sorption rate constant can be obtained from the model according to Eg. 5:

$$\frac{t}{q_t} = \frac{1}{k_2 q_e^2} + \frac{1}{q_e} t, \tag{5}$$

where k_2 (g/(μmol min) is the pseudo-second-order rate constant; q_t (μmol/g) and q_e (μmol/g) are the amount of dye adsorbed at time t and at equilibrium, respectively. k_2 and q_e can be calculated from the intercept and slope. The plot of t/q_t vs t shows a linear relationship for Purolite A 500PS (Fig. 5c) and Macronet MN 200 (Fig. 5d). The calculated q_e and k_2 values are given in Table 4. The correlation coefficients (R^2) are high, in the range of 0.9866–0.9988, confirming a good agreement of the kinetic model with experimental data.

The pseudo-second-order rate constants k_2 and the equilibrium adsorption capacity q_e calculated for the macroporous Purolite A 500PS were greater than those for the hypercrosslinked Macronet MN 200 (Table 4). The influence of temperature on CuPc dye sorption on the Macronet MN 200 is higher than that on Purolite A 500PS. With increase in temperature from 293K to 313K, the calculated k_2 values for

CuPc dye sorption on Purolite A 500PS are only 2.7 times higher (148.6 and 399.7 g/(μmol min), respectively) and q_e values are 1.7 times lower, while the k_2 values calculated for Macronet MN 200 are even 12 times higher (3.66 and 44.53 (μmol min)) and q_e increases 3.5 times. This temperature effect determined for Macronet MN 200 is called the activated chemical adsorption. The fact that the dye sorption capacity depends on temperature is primarily concerned with the occurrence of diffusion [34, 35].

From the kinetic parameter k_2 at different temperatures, the activation energies, representing the minimum energy that the dye-sorbent system should have for sorption to proceed, were estimated using the Arrhenius relationship [36]:

$$\ln k_2 = \ln A - \frac{E_a}{RT}, \tag{6}$$

where E_a is the Arrhenius activation energy of adsorption, A is the Arrhenius factor, R is the gas constant equal to 8.314 J/mol K, and T is the solution temperature, K. The obtained ln k_2 straight lines with a slope $- E_{a-k2}$/R and positive activation energies for Purolite A 500PS and Macronet MN 200 34.27 and 93.99 kJ/mol, respectively, comply with the limits of the meso- to macroporous sorbents (40 kJ/mol) and microporous sorbents (100 kJ/mol) [32].

The adsorbate transport from the solute to the surface of the adsorbent particles occurred in several steps two of which appear to control the sorption rate: mass transfer in either the bead (intraparticle diffusion) or the external diffusion (boundary layer diffusion), whichever is slower [37, 38]. Since the experiments were carried out in a rapidly stirred 400 rev/min batch reactor when the boundary layer diffusion should be immaterial, the role of the polymeric matrix structure on the sorption of CuPc dye can be dealt with the initial rate of intraparticle diffusion calculated from Eq. 7 [39–42]:

$$q_t = k_i t^{0.5} + A, \tag{7}$$

where q_t is the amount of dye on the surface of the sorbent at time t (μmol/g), k_i is the intraparticle diffusion rate constant (μmol/g min$^{0.5}$), t is the time (min) and A is the intercept (μmol/g). The values of intercept A represent the boundary layer thickness, thus, the larger the intercept the greater is the boundary layer effect. According to this model, the plot of q_t versus the square root of time ($t^{0.5}$) should be linear if intraparticle diffusion is involved in adsorption and if these

Table 4. **Pseudo-second-order rate constants and equilibrium sorption values for CuPc dye sorption on Purolite A 500PS and Macronet MN 200 obtained at various temperatures**

T(K)	Purolite A 500PS			Macronet MN 200		
	k_2, g/μmol min	q_e, μmol/g	R^2	k_2, g/μmol min	q_e, μmol/g	R^2
293	148.6	86.9	0.9984	3.669	2.3	0.9919
303	387.7	60.1	0.9866	32.933	6.9	0.9988
313	399.7	50.4	0.9916	44.532	8.1	0.9920

Table 5. **Intraparticle diffusion rate constant k_i and boundary layer thickness (A) for CuPc dye sorption on Purolite A 500PS and Macronet MN 200 obtained at various temperatures**

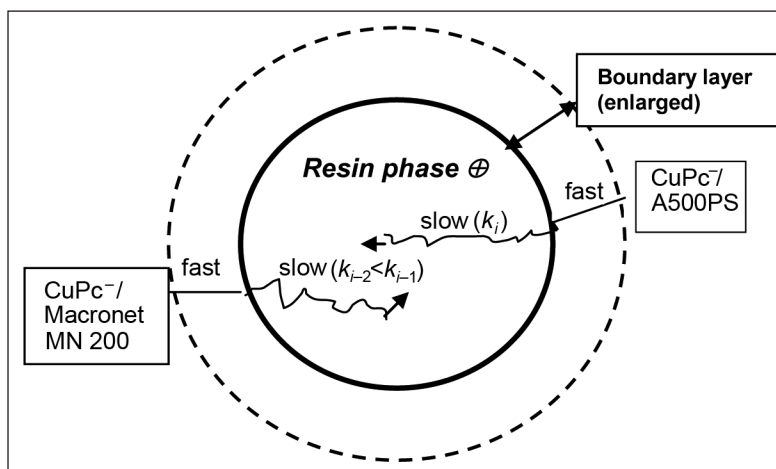| T (K)	Purolite A 500PS	Macronet MN 200		
	k_i, µmol/g min$^{0.5}$	k_{i-1}, µmol/g min$^{0.5}$	k_{i-2}, µmol/g min$^{0.5}$	A, µmol/g
293	6.2	0.35	0.0433	1.533
303	4.0	1.20	0.0433	5.433
313	3.0	1.41	0.0433	6.733

Fig. 6. Limitation of CuPc dye diffusion in the sorption by Purolite A 500PS and Macronet MN 200

lines pass through the origin then intraparticle diffusion is the rate-controlling step.

The plot of q_t against $t^{0.5}$ for CuPc dye sorption on Purolite A 500P is a straight line passing through the origin (Fig. 5e) which confirms that the sorption process is limited only by transport of CuPc dye within the macro and meso pores of the anion exchanger (intraparticle diffusion). Contrary to the CuPc sorption on Purolite A 500PS anion exchanger, the plot of q_t against $t^{0.5}$ for CuPc dye sorption on Macronet MN 200 was multi-linear and might present different stages of intraparticle diffusion in the macro-, meso-, and micropores structure of the sorbent [18]. The first linear portion in the temperature range of 293–333K was ascribed to the intraparticle diffusion through macro- and mesopores (Fig. 5f). The second stage may be regarded as the diffusion through micropores, and, of course, this stage is followed forthwith by the establishment of equilibrium. The slope of the linear plot of q_t against $t^{0.5}$ for the Purolite A 500PS anion exchanger (k_i) and the first and second linear portion of the plot q_t against $t^{0.5}$ for Macronet MN 200 k_{i-1} and k_{i-2}, respectively, were used to derive values for the intraparticle diffusion rate parameter given in Table 5. The correlation coefficients (R^2) for the intraparticle diffusion model are 0.9696–0.9944 for the CuPc dye sorption on Purolite A 500PS and 0.9199–0.9964 for CuPc dye sorption on Macronet MN 200. This indicates that CuPc dye adsorption on both sorbents proceeds according to the intraparticle diffusion model.

Although the surface area and pore volume of Macronet MN 200 are significantly higher than those of Puro-

lite A 500PS (Table 1), the intraparticle diffusion rate constants k_i data of the latter were found to be markedly higher than k_{i-1} for MN 200 (Table 5). The surface charges of the sorbents at pH 3.0 are not significantly different: the zeta potential of Purolite A 500PS is approximately 30 mV and that of Macronet MN 200 is 25 mV [12, 42], the above mentioned data may be ascribed to the ion exchange reaction between the CuPc dye anion and the protonated quarternary amino groups ($-N^+(CH_3)_3OH^-$) of Purolite A 500PS rather than to the electrostatic interaction. The values of $k_{i-1} > k_{i-2}$ (Table 5) calculated for CuPc dye sorption on Macronet MN 200 confirmed that the CuPc dye diffusion resistance in micropores is larger than that in macro- and mesopores. Besides, the CuPc dye intraparticle diffusion on Macronet MN 200 is affected by boundary layer thickness A that increases with temperature increase (Table 5). Fig. 6 illustrates the limitation of CuPc dye diffusion in the sorption by Purolite A 500PS and Macronet MN 200.

On the other hand, the effect of temperature on the intraparticle diffusion rate was quite different as shown in Table 5: k_i for Purolite A 500PS shows a tendency for decrease with increase in temperature and k_{i-1} for MN 200 shows a tendency for increase (Table 5).

The activation energies, representing the minimum energies needed for CuPc dye intraparticle sorption to proceed on Macronet MN 200 (E_{ki-1}) and on Purolite A 500PS (E_{ki}) were +52.17 and –26.65 kJ/mol, respectively, which confirms that CuPc dye penetration into the Macronet MN 200 bead is slower when compared to the penetration into the Purolite A 500PS bead.

CONCLUSIONS

The comparison of two polystyrene divinylbenzene matrix sorbents: the macroporous strong base anion exchanger Purolite A 500PS and hypercrosslinked non-fuctionalized Macronet MN 200 showed that Purolite A 500PS is substantially more effective for the sorption of copper phthalocyanine dye – Acid Blue 249 (CuPc) than Macronet MN 200. The amount of CuPc dye sorbed at equilibrium on Purolite A 500PS and on Macronet MN 200 was 86.9 µmol/g and 2.3 µmol/g, respectively. FTIR spectra of unloaded and CuPc dye loaded both the Purolite A 500PS and Macronet MN 200 revealed that in the CuPc dye anion sorption the protonated quarternary amino groups of Purolite A 500PS and phenolic groups of Macronet MN 200 are involved.

The experimental kinetic data can be well described by the pseudo-second-order and intraparticle diffusion models. The pseudo-second-order rate constants k_2 and the equilibrium adsorption capacity q_e calculated for Purolite A 500PS were greater than those for Macronet MN 200. The dependence of k_2 and q_e values on increase in temperature obtained for CuPc dye sorption on both Purolite A 500PS and Macronet MN 200 is concerned with the occurrence of CuPc dye anion diffusion. The sorption on Purolite A 500PS is limited by CuPc dye diffusion within the macro- and mesopores (k_i), whereas on Macronet MN 200 it is limited by CuPc dye diffusion within the macro- and mesopores (k_{i-1}) and micropores (k_{i-2}) with higher intraparticle diffusion rate constant for Purolite A 500PS (k_i) than that for Macronet MN 200 (k_{i-1}). The CuPc dye diffusion resistance in micropores of the Macronet MN 200 bead is significantly larger than that in macro- and mesoropores ($k_{i-1} > k_{i-2}$). Significantly higher activation energy values obtained for intraparticle diffusion of Macronet MN 200 than those for Purolite A 500PS confirm that the CuPc dye diffusion in micropores of the Macronet MN 200 bead diminishes the CuPc dye intraparticle diffusion rate constant.

ACKNOWLEDGEMENTS

References

1. V. Dulman, C. Simion, A. Bârsănescu, I. Bunia, V. Neagu, *J. Appl. Polym. Sci.*, **113**, 615 (2009).
2. S. Kärcher, A. Kornmüller, M. Jekel, *Dyes Pigm.*, **51**, 111 (2001).
3. M. Wawrzkiewicz, Z. Hubicki, *J. Hazard. Mater.*, **164**, 502 (2009).
4. M. Leszczynska, Z. Hubicki, *Desalin. Water Treat.*, **2**, 156 (2009).
5. M. Wawrzkiewicz, Z. Hubicki, *Chem. Eng. J.*, **150**, 509 (2009).
6. M. Wawrzkiewicz, Z. Hubicki, *J. Hazard. Mater.*, **172**, 868 (2009).
7. M. Greluk, Z. Hubicki, *J. Hazard. Mater.*, **172**, 280 (2009).
8. S. Dragan, M. Cristea, A. Airinei, I. Poinescu, C. Luca, *J. Appl. Polym. Sci.*, **55**, 421 (1995).
9. M. Wawrzkiewicz, *Environ. Technol.*, **32**, 445 (2011).
10. K. Dorfner (ed.), *Ion Exchangers*, Walter de Gruyter, Berlin, New York (1991).
11. M. H. Tai, B. Saha, M. Streat, *React. Func. Polym.*, **41**, 149 (1999).
12. N. A. Penner, P. N. Nesterenko, *Anal. Commun.*, **36**, 199 (1999).
13. M. P. Baya, P. A. Siskos, *J. AOAC Inter.*, **83**, 579 (2000).
14. M. Streat, L. A. Sweetland, *React. Func. Polym.*, **35**, 99 (1997).
15. R. M. C. Sutton, S. J. Hill, P. Jones, *J. Chromatogr. A*, **789**, 389 (1997).
16. M. P. Tsyurupa, O. G. Tarabaeva, A. V. Pastukhov, V. A. Davankov, *Inter. J. Polym. Mater.*, **52**, 403 (2003).
17. V. A. Davankov, M. P. Tsyurupa, N. N. Alexienko, *J. Chromatogr. A*, **1100**, 32 (2005).
18. C. Valderrama, J. L. Cortina, A. Farran, F. Gamisans, F. X. de las Heras, *React. Funct. Polym.*, **68**, 679 (2008).
19. C. Valderrama, J. L. Cortina, A. Farran, X. Gamisans, F. X. de las Heras, *React. Funct. Polym.*, **68**, 718 (2008).
20. E. Belston, D. Naden, *Proceedings of the International Conference on Water and Textiles*, Huddersfield (1999).
21. K. Hunger (ed.), *Industrial Dyes. Chemistry, Properties, Application*, Wiley-VCH, Weinheim (2003).
22. K. Petritsch, J. J. Dittmer, E. A. Marseglia, et al., *Sol. Energy. Mater. Sol. Cells*, **61**, 63 (2000).
23. M. E. Wieder, D. C. Hone, M. J. Cook, M. M. Handsley, J. Gavrilovic, D. A. Russell, *Photochem. Photobiol. Sci.*, **5**, 727 (2006).
24. R. Aroca, H. Bolourchi, D. Battisti, K. Najafi, *Langmuir*, **9**, 3138 (1993).
25. J. Souto, J. A. de Saja, M. I. Gobernado-Mitre, M. L. Rodriguez, R. Aroca, *Sens. Actuators, B*, **16**, 306 (1993).
26. M. I. Gobernado-Mitre, L. G. Tomilova, R. Aroca, J. A. De-Saja, *J. Mol. Struct.*, **297**, 49 (1993).
27. G. Laing, *Rev. Prog. Color.*, **21**, 56 (1996).
28. O. N. Kononova, N. G. Goryaeva, O. V. Dychko, *Natural Science*, **1**, 166 (2009).
29. S. Seelan, M. S. Agashe, D. Srinivas, S. Sivasanker, *J. Mol. Catal. A: Chem.*, **168**, 61(2001).
30. G. Wronski, S. Pasieczna-Patkowska, Z. Hubicki, *Eur. Phys. J. Spec. Top.*, **154**, 377 (2008).
31. E. Kazlauskienė, D. Kaušpėdienė, A. Gefenienė, A. Selskienė, R. Binkienė, *Chemija*, **20**, 69 (2009).
32. V. J. Inglezakis, A. A. Zorpas, *Desalin. Water Treat.*, **39**, 149 (2012).
33. Y. S. Ho, *J. Hazard. Mater.*, **B136**, 681 (2006).

34. W. J. Weber, J. C. Morris, *J. Sanitary Eng. Div. Am. Soc. Civ. Eng.*, **89**, 31 (1963).

35. K. V. Kumar, V. Ramamurthi, S. Sivanesan, *J. Colloid Interface Sci.*, **284**, 14 (2005).

36. A. Özcan, M. Öncü, A. S. Özcan, *J. Hazard. Mater.*, **129B**, 244 (2006).

37. N. Kannan, M. M. Sundaram, *Dyes Pigm.*, **51**, 25 (2001).

38. S. Wang, H. Li, *Dyes Pigm.*, **72**, 308 (2007).

39. M. A. M. Kharaisheh, Y. S. Al-Degs, S. J. Allen, M. N. Ahmad, *Ind. Eng. Chem. Res.*, **41**, 1651 (2002).

40. S. J. Allen, G. McKay, K. Y. H. Khader, *Environ. Pollut.*, **56**, 39 (1989).

41. M. S. Chiou, G. S. Chuang, *Chemosphere*, **62**, 731 (2006).

42. I. H. Yoon, X. Meng, Ch. Wang, K. W. Kim, S. Bang, E. Choe, L. Lippincott, *J. Hazard. Mater.*, **164**, 87 (2009).

D. Kaušpėdienė, E. Kazlauskienė, R. Česūnienė, A. Gefenienė, R. Ragauskas, A. Selskienė

FTALOCIANINO DAŽIKLIO PAŠALINIMAS IŠ RŪGŠTINIŲ TIRPALŲ NAUDOJANT POLISTIRENO-DIVINILBENZENO SORBENTUS

S a n t r a u k a

Tirta dažiklio – vario ftalocianino Acid Blue 249 (CuPc) – pašalinimas iš vandens tirpalų naudojant skirtingos tinklinės struktūros polistireno-divinilbenzeno sorbentus: makroporinį stipriai bazinį Purolite A 500PS ir inertinį hipertinklinį Macronet MN 200. Statinėmis sąlygomis nustatyta sorbcijos ir kinetikos priklausomumas nuo CuPc tirpalo pH, temperatūros. Sorbentų paviršių tekstūros vertintos elektroniniu skenuojančiu mikroskopu. Lyginant pradinių ir prisotintų CuPc sorbentų funkcinių grupių pokyčius FTIR spektroskopijos metodu nustatyti charakteringi CuPc anijono sorbcijos mechanizmai: jonų mainai dalyvaujant Purolite A 500PS ketvirtinėms amino grupėms ir elektrostatinė sąveika su Macronet MN 200 fenolinėmis grupėmis. Sorbcijos kinetika patikimai koreliuoja su vidinės difuzijos ir pseudoantrojo laipsnio kinetikos modeliais. Apskaičiuotos vidinės difuzijos (E_{a-ki}) ir cheminės sorbcijos (E_{a-k2}) aktyvacijos energijos naudojant Arenijaus lygtį. Nustatyta, kad CuPc sorbciją Purolite A 500PS limituoja vidinė difuzija, o Macronet MN 200 – vidinė difuzija, priklausomai nuo porų apimties ir paribio sluoksnio storio.

Dažiklį CuPc efektyviau sorbuoja Purolite A 500PS nei MN 200: atitinkamai 86,9 mmol/g ir 2,3 mmol/g.